applied sciences

MDPI

Article

Analysing Mouse Skin Cell Behaviour under a Non-Thermal kHz Plasma Jet

Andrea Jurov [1,2], Špela Kos [3], Nataša Hojnik [1], Ivana Sremački [4], Anton Nikiforov [4], Christophe Leys [4], Gregor Serša [3] and Uroš Cvelbar [1,*]

1 Jožef Stefan Institute, Jamova cesta 39, 1000 Ljubljana, Slovenia; andrea.jurov@ijs.si (A.J.); natasa.hojnik@ijs.si (N.H.)
2 Jožef Stefan International Postgraduate School, Jamova cesta 39, 1000 Ljubljana, Slovenia
3 Department of Experimental Oncology, Institute of Oncology, Zaloška cesta 2, 1000 Ljubljana, Slovenia; skos@onko-i.si (Š.K.); gsersa@onko-i.si (G.S.)
4 Department of Applied Physics, Ghent University, Sint-Petersnieuwstraar 41, 9000 Gent, Belgium; ivana.sremacki@ugent.be (I.S.); anton.nikiforov@ugent.be (A.N.); christophe.leys@ugent.be (C.L.)
* Correspondence: uros.cvelbar@ijs.si

Abstract: Plasma jets are extensively used in biomedical applications, particularly for exploring cell viability behaviour. However, many experimental parameters influence the results, including jet characteristics, secondary liquid chemistry and protocols used, slowing research progress. A specific interest of the presented research was skin cell behaviour under a non-thermal kHz plasma jet—a so-called cold plasma jet—as a topical skin treatment. Our research was focused on in vitro mouse skin cell direct plasma treatment with argon as an operating gas. The research was complemented with detailed gas-phase diagnostics and liquid-phase chemical analysis of the plasma and plasma-treated medium, respectively. The obtained results showed that direct plasma jet treatment was very destructive, leading to low cell viability. Even with short treatment times (from 35 s to 60 s), apoptosis was observed for most L929 murine fibroblasts under approximately the same conditions. This behaviour was attributed to plasma species generated from direct treatment and the types of cell lines used. Importantly, the research exposed important points that should be taken under consideration for all further research in this field: the urgent need to upgrade and standardise existing plasma treatment protocols of cell lines; to monitor gas and liquid chemistries and to standardise plasma discharge parameters.

Keywords: atmospheric pressure plasma jet; cell viability; plasma-treated media; reactive species; optical emission spectroscopy

Citation: Jurov, A.; Kos, Š.; Hojnik, N.; Sremački, I.; Nikiforov, A.; Leys, C.; Serša, G.; Cvelbar, U. Analysing Mouse Skin Cell Behaviour under a Non-Thermal kHz Plasma Jet. *Appl. Sci.* **2021**, *11*, 1266. https://doi.org/10.3390/app11031266

Academic Editor: Daniela Boehm
Received: 5 December 2020
Accepted: 27 January 2021
Published: 30 January 2021

1. Introduction

Non-thermal atmospheric pressure plasmas (APPs) are widely used for various applications. They show great potential in the field of medicine [1–3] because of properties such as low gas temperature, high generation rate of reactive species, affordability and simple setup compared to low-pressure plasma systems. Different frequencies can ignite plasma. The most widely used configurations are simple kHz driven jets [4–9], but microwave [10] and radio frequency [11,12] driven jets have also been reported. This type of plasma contains short-lived free radicals, charged species, neutral species, reactive oxygen and nitrogen species (RONS), UV radiation, and electric fields; all of which can influence biological samples [9].

Assuming RONS influence living cells the most out of all plasma components, their production is of interest for this research [13]. In the gas phase, plasma ionises and excites species from the ambient air which recombine into RONS. These then reach the cell culture medium and interact with liquid components. Gaseous RONS quickly recombine, leading to the formation of other species, such as nitrites (NO_2^-), nitrates (NO_3^-), hydrogen

peroxide (H_2O_2) and peroxynitrite ($ONOO^-$), of which NO_2^- and H_2O_2 are the easiest to detect and quantify.

Based on their presence in a given liquid medium, some assumptions about RONS dynamics can be made. Depending on the dosage of nitrite (NO_2^-) and hydrogen peroxide (H_2O_2), one can obtain both positive (cell proliferation, cell differentiation, angiogenesis) and negative (apoptosis, necrosis, growth arrest) effects on cells [1,2,9,14]. Both positive and negative effects can be useful in different applications. For example, in cancer treatment, it is useful to induce damage to target cells, but in open wound treatment, cells should not be damaged at all.

Depending on the required result, there are different approaches to treating cells: direct and indirect. The direct approach involves direct plasma treatment of biological cells while they are inside the cell culture medium. Indirect plasma treatment means that a liquid medium is treated with plasma (a plasma-treated medium (PAM)) and is subsequently added to the cells. One difference between these approaches is the species—produced in the gas phase—that reach and interact with the cells [15]. In the case of direct plasma treatment, both short- and long-lived species will interact with cells. In contrast, with an indirect approach, only long-lived species produced in the gas phase will interact with cells. However, this does not imply that there are no short-lived species inside the liquid; they form again when long-lived species decompose and recombine. Both direct and indirect plasma treatments influence cell processes and morphology changes [16].

This research aimed to create a simple single-electrode, kHz-driven plasma jet and examine its effect on L929 murine fibroblast cells. The motive was to explore this type of plasma jet's usability for topical skin treatment—and consequently for wound healing or gene delivery—and then compare this source with other similar approaches and investigations. To do so, we chose argon plasma, which is relatively unexplored, for direct cell treatment on healthy mouse skin cells. Direct plasma treatment was chosen in order to shorten the procedure, as indirect plasma-treated cells must be incubated in PAM for at least 24 h. Argon was chosen over helium gas because of its affordability and processing sustainability. Moreover, under the same conditions, argon plasma has higher electron density but lower electron temperature, which was considered an advantage for direct cell treatment [17].

2. Materials and Methods

2.1. Plasma Jet Configuration and Power Source Characterisation

A non-thermal APP in the form of a jet (powered by a kHz source) was used for this research. The plasma jet was constructed as a single electrode jet with no additional grounding. Therefore, a plasma plume could be formed inside a 2 mm diameter glass tube. Depending on the gas type, flow could reach up to 1.5 cm in length, measured from the end of the glass orifice outward. A schematic representation of this setup is shown in Figure 1. Diagnostic measurements (optical emission spectroscopy (OES) and I-V characterisation) were conducted while the plasma operated over a non-grounded distilled water target. This target was chosen to allow the gas-phase diagnostics to be taken closer to the cell treatment, as the cells are dispersed inside a liquid medium. Distilled water was placed in a cylindrical container of 6280 mm^3 volume at 2 cm distance from the end of the jet's glass tube.

The jet was powered by a 20 kHz power source (Amazing PMV500, Information Unlimited, Amherst, NH, USA). Based on preliminary tests, parameters were fixed at a maximum frequency and 60% power input in low operating mode (0.24 W). These conditions produced the most stable argon plasma. Current and voltage were stable sinusoidal waves without any arbitrary peaks.

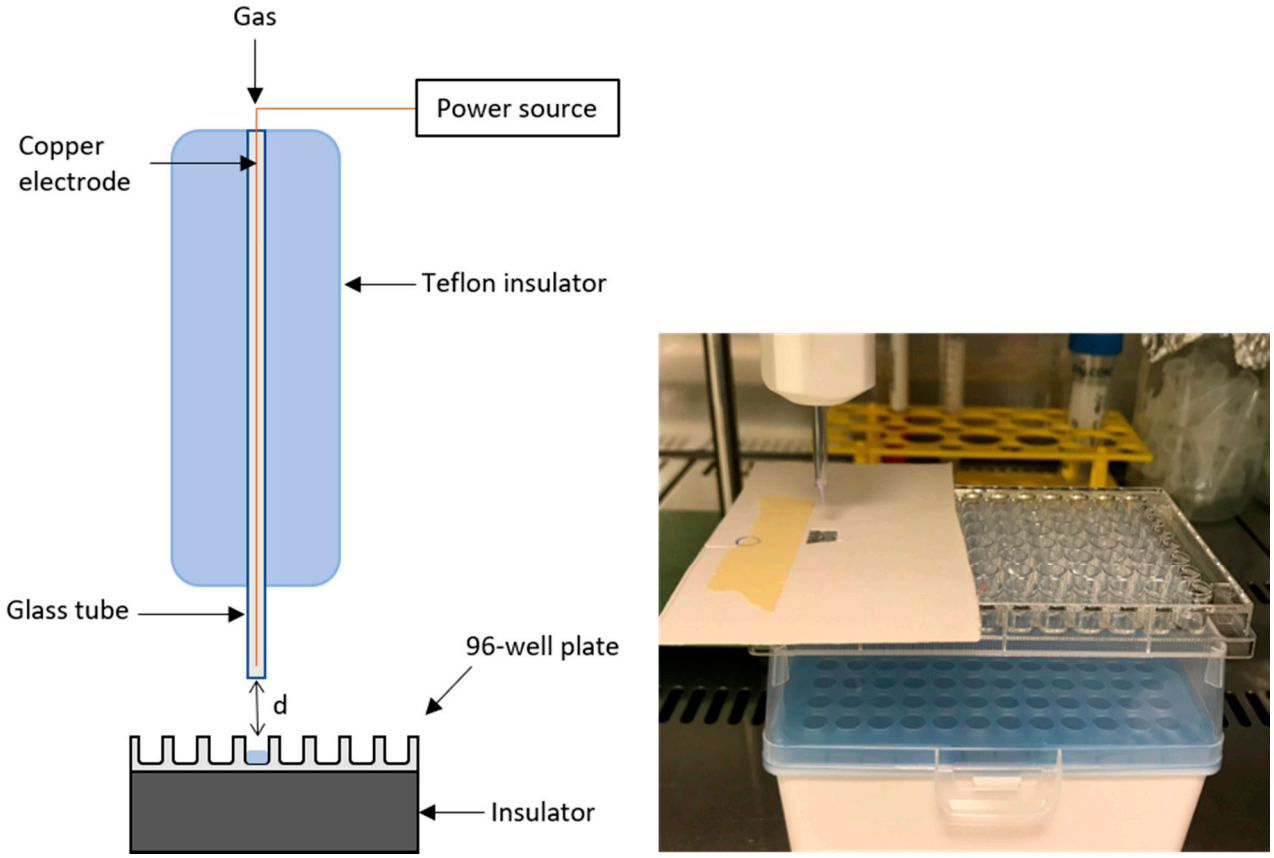

Figure 1. Schematic representation (**left**) and photograph (**right**) of the simple plasma jet system and setup for an in vitro cell treatment.

The voltage and current of the power source were monitored in real time, just before the jet. For this purpose, an HV probe (Tektronix P6105A, Tektronix Inc., Beaverton, OR, USA) and a current monitor (Pearson 2877, Pearson Electronics Inc., Palo Alto, CA, USA) were coupled with an oscilloscope (Picoscope 3204d, Pico Technology Ltd., Cambridgeshire, UK). Waveforms were monitored to ensure they were stable under the experiments' conditions but were not monitored throughout the experiments on the cell culture medium.

2.2. Gas-Phase Diagnostics

Diagnostics of plasma in the gas phase is important for monitoring the excited species' production and understanding the principles behind plasma ionisation. For this purpose, both OES and time-resolved ICCD (Intensified Charged Couple Device) imaging were used.

For OES measurements, we used broad-range, spatially-resolved and time-resolved spectroscopy. The broad-range spectra provided insight into the species that were excited in plasma, whereas the spatially-resolved spectra enabled monitoring of excited species' intensities produced in plasma, with respect to the distance from the jet. The time-resolved spectra exposed information about how chosen species form throughout one period. To obtain the broad-range and spatially-resolved spectra, an Avantes spectrometer (Avantes BV, Apeldoorn, The Netherlands) with 0.05 nm resolution was used. For time-resolved spectroscopy, a 0.75 m Zolix spectrometer (Zolix Instruments Co., LTD, Beijing, China) with a grating of 1200 grooves/mm (blazed on 500 nm) was used.

ICCD imaging was utilised to gain an insight into 'bullet' formation and propagation within the waveform, along with filament production. For these measurements, a Hamamatsu ICCD camera was used (Hamamatsu Photonics K.K., Naka-ku, Hamamatsu City,

Japan). Imaging was time-resolved, and it covered the whole period. Images were obtained with an exposure time of 100 ns and at one integration.

2.3. In Vitro Cell Experiments

To investigate the effects of a kHz plasma jet on biomedical samples with a focus on skin treatment, in vitro experiments were performed with L929 murine fibroblasts. The discharge parameters were constant throughout all experiments. The argon flow rate was 1 SLM, and the source's power was fixed at 60% of the maximum available power. Different treatment times were used; more precisely, 10 s, 35 s and 60 s. The distance between the plasma jet and cell medium was 10 mm, 15 mm and 20 mm, respectively, measured from the end of the jet's glass tube to the surface of the well plate (marked as d in Figure 1). This distance was measured from the jet to the top of the well plate rather than the liquid surface, for easier monitoring. Another 7 mm should be added to these values to denote the distance from the point plasma exists in the glass tube and mixes with the ambient air to the surface of the cells dispersed in the culture medium. The distances were chosen based on the position of the plasma plume, which was either touching the surface of the substrate or its immediate or far afterglow region.

Since all in vitro cell experiments required a controlled sterile environment, they were conducted inside a laminar cabinet (Iskra PIO M12V). Laminar is essentially a large metal box, and it influences plasma intensity by acting as a grounding electrode under the sample. To mitigate this effect, a 10 cm tall dielectric was placed under the well plate. Additionally, single well treatment was assured by a barrier plate with a circular hole which was placed on top of the well plate. This provided full control over jet species in the far afterglow region and prevented their expansion to neighbouring wells. Both the dielectric under a sample and the barrier placed on top of the well-plate are shown in Figure 1.

2.4. Cell Lines

The L929 murine fibroblasts (American Type Culture Collection, ATCC, Manassas, VA, USA) were cultured in an advanced minimum essential medium (AMEM) (Gibco, Thermo Fisher Scientific, Waltham, MA, USA), supplemented with 5% fetal bovine serum (FBS; Gibco), 10 mL/l L-glutamine (GlutaMAX; Gibco), 100 U/mL penicillin and 100 µg/mL streptomycin (Pen-Strep, Sigma-Aldrich, Merck, St. Louis, MO, USA) in a 5% CO_2 humidified incubator at 37 °C.

Cell Viability Assay

For cell viability assay, L929 cells were trypsinised and counted. Prior to treatment, cells were resuspended in the cell medium (MEM (Minimum Essential Medium) without phenol red, Gibco) and 1000 L929 cells/well were placed in 96-well plates (Corning Incorporated, Corning, NY, USA) in a 0.1 mL cell culture medium. Immediately after the cell suspension was placed in plates, plasma treatment was performed as described above. Cells were incubated at 37 °C in a 5% CO_2 humidified incubator for up to three days. 24 h and 72 h after treatment, 10 µL of Presto Blue® viability reagent (Thermo Fisher Scientific, Waltham, MA, USA) was added to the wells, and 1 h later fluorescence intensity was measured by a microplate reader (Cytation 1, BioTek Instruments, Winooski, VT, USA). The percentage of viable cells was calculated and normalised to the untreated control group. Three replicates were used for each experimental group; each experiment was repeated three times. For statistical analysis, GraphPad Prism Software (version 9.0.0) was used. Data are presented as the arithmetic mean (AM) ± the mean standard error (SE). One-way ANOVA followed by the Tukey test for multiple comparisons was used for the determination of significant differences ($p < 0.05$ *, $p < 0.01$ **, $p < 0.001$ ***, $p < 0.0001$ ****) between groups.

2.5. Liquid-Phase Chemistry Analysis

Plasma-induced modifications and the liquid chemistry of culture medium MEMs were analysed using different analytical techniques. Identical plasma treatment conditions were employed as in the case of in vitro cell experiments. Immediately following treatments (0 h), the treated MEM's pH and conductivity were measured with PC 52+ DHS® (XS instruments, Italy). To obtain more information about the dynamics of the plasma-induced liquid chemistry, colourimetric tests were performed to evaluate the presence of NO_2^- and H_2O_2 using a plate reader in UV-VIS spectrometry mode (Spark 10M, Tecan, Switzerland) at 0 h, 24 h and 72 h after the treatments. The presence of NO_2^- was determined with standard Griess reagent assay (Griess reagent system; Promega, Madison, WI, USA) measuring absorbance values at 540 nm. H_2O_2 concentrations were tested with a ferric-xylenol orange complex (xylenol orange, sorbitol and ammonium iron sulphate; Sigma-Aldrich), which was added to the treated MEM. Following the chemical reaction, the absorbance of the solution was measured at 560 nm. Tests were performed in multiple independent experiments and results replicated. The obtained results were statistically analysed with 2-way ANOVA (GraphPad Prism, San Diego, CA, USA).

3. Results

3.1. Gaseous Plasma Characteristics

Broad-range spectra (Figure 2a) confirmed the presence of the usual species for an APP generated within argon gas; excited argon species from the ionisation of the working gas, and the reactive species of nitrogen (second positive band—$C^3\Pi_u \rightarrow B^3\Pi_g$), along with OH groups coming from the ambient air filled with water vapour. Given that the OH peak did not overlap with other lines, it was used to determine plasma gas temperature with LIFbase Database and spectral simulation programme (Version 2.1) [12]. The temperature measured was 318 K while plasma was in contact with a water target as described in Section 2.2.

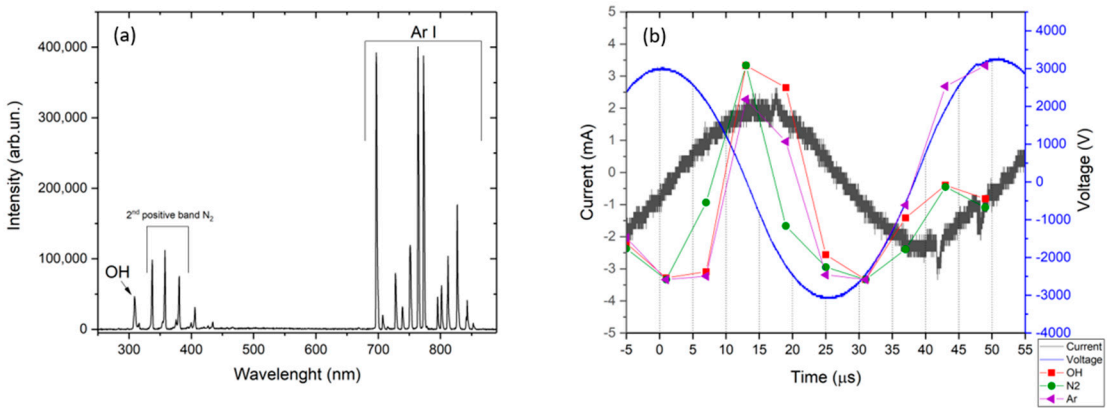

Figure 2. Broad-range emission spectrum of Ar plasma operated above a non-grounded water target (**a**) and time-resolved optical emission spectroscopy (OES) during one period (**b**).

Spatially-resolved spectra were measured at the exit of the glass tube and the plasma plume's end; approximately 1 cm apart. This distance was also the length of the used plasma plume under all experimental conditions. The spectra exhibited no specific difference when the intensity was normalised to 1 (presented in the supplementary file). Intensity normalisation allowed spectra intensity comparison, and did not influence the line intensity ratio within each recorded spectrum. Based on this result, we were confident that excited species from the gas phase delivered to the cell medium were similar at each distance used for direct cell treatment.

Intensities of OH (309 nm), N_2 (391 nm) and Ar (696 nm) were monitored throughout one period by time-resolved spectroscopy. These data were paired with I-V characteristics in Figure 2b. Our power source operated at an average maximum value of 3.4 kV and

2.8 mA at chosen discharge parameters. One period lasted for 50 µs, where maximum voltage values were fixed at 0 and 50 µs. All monitored plasma species exhibited similar behaviour. Their excitation intensity increased as the voltage dropped, and later decreased as the voltage reached its minimum value. A subsequent increase in the intensity started when voltage rose. However, Ar time-intensity more than doubled compared to the intensities of OH and N_2. This behaviour is connected to plasma 'bullet' streamer and filament formation and propagation, which ICCD images highlight in Figure 3 [18–20]. Plasma streamer formation starts around 12 µs when the voltage changes from positive to negative, and propagates until the voltage reaches its minimum value. Then, the ionisation shifts and at around 37 µs filaments start to appear, gaining their maximum intensity soon after. Time-resolved OES indicated that Ar plays the most important role in filament formation, with OH and N_2 in secondary roles.

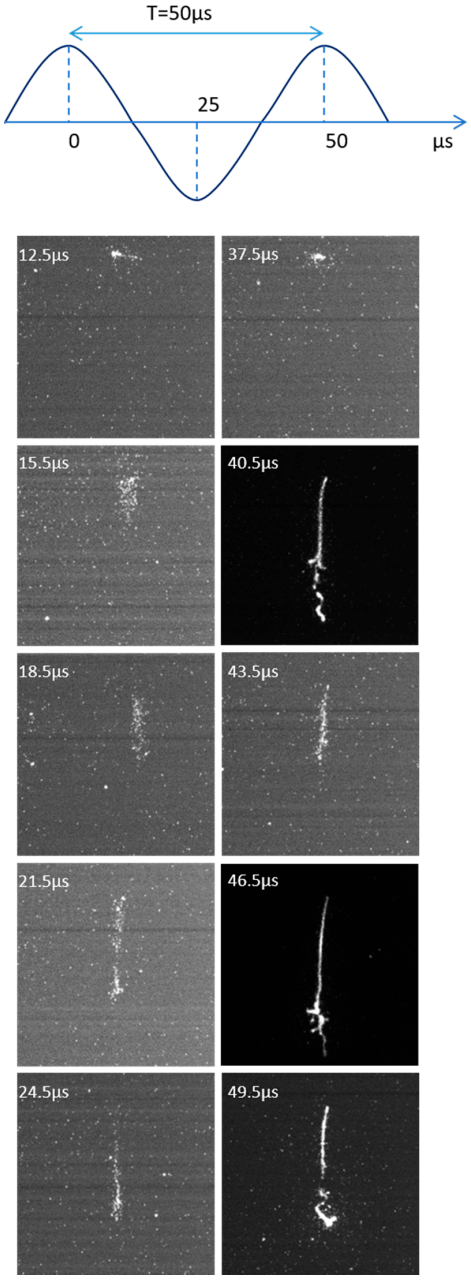

Figure 3. Plasma ionisation process. Propagation of a plasma bullet type of ionisation (**left**), from 12 µs to 25 µs, and formation of filaments (**right**), from 37 µs to 50 µs.

3.2. Plasma-Liquid Chemistry

To fully understand the plasma jet impact on cells in a liquid culture medium, the potential plasma-induced modifications in liquid chemistry need to be evaluated in detail. Firstly, as the liquid culture medium's pH is one of the most important factors that significantly influence cell viability, the pH of MEM was measured immediately after exposure to plasma. The results demonstrated no significant discrepancies from the non-treated sample's values or control (Figure 4). Thus, it was concluded that the pH level was not a contributing factor. Along with pH, conductivity was measured. As in the results obtained from pH measurements, conductivity exhibited similar stability. Data are presented in the supplementary file.

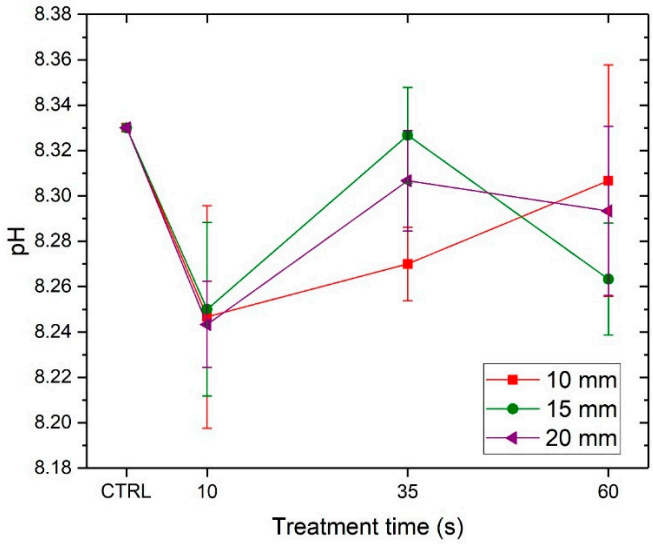

Figure 4. pH of plasma treated MEM measured right after treatment. Results are presented as mean values ± SEM (two-way ANOVA, Dunnett's post-tests; n = 3).

In contrast to the findings obtained for pH and conductivity measurements, the plasma treatments induced a slight increase in the concentrations of NO_2^- and H_2O_2. Figure 5a displays the concentrations of NO_2^- obtained immediately after treatment. As demonstrated from the results, the concentrations gradually increased with shorter distances between the plasma ignition point and MEM surface and longer exposure times. The maximum NO_2^- value (i.e., 10.5 µM) was measured at a distance of 10 mm after 60 s of exposure. Long distances led to negligible increases in NO_2^- concentrations. Similar trends were also observed for results obtained 24 h and 72 h after treatments (Figure 5c,e), where, generally, a small increase in NO_2^- concentration was noted. The shortest treatment distance and longest exposure time also led to the formation of the highest H_2O_2 concentration directly after plasma treatment (Figure 5b). A 60 s exposure of MEM to plasma at 10 mm distance resulted in the generation of 25.9 µM of H_2O_2. In contrast, concentrations of 19.5 µM and 6.3 µM were recorded at treatment distances of 15 mm and 20 mm, respectively. Unlike NO_2^-, H_2O_2 concentrations significantly shrank or completely disappeared after 24 h and 72 h (Figure 5d,f).

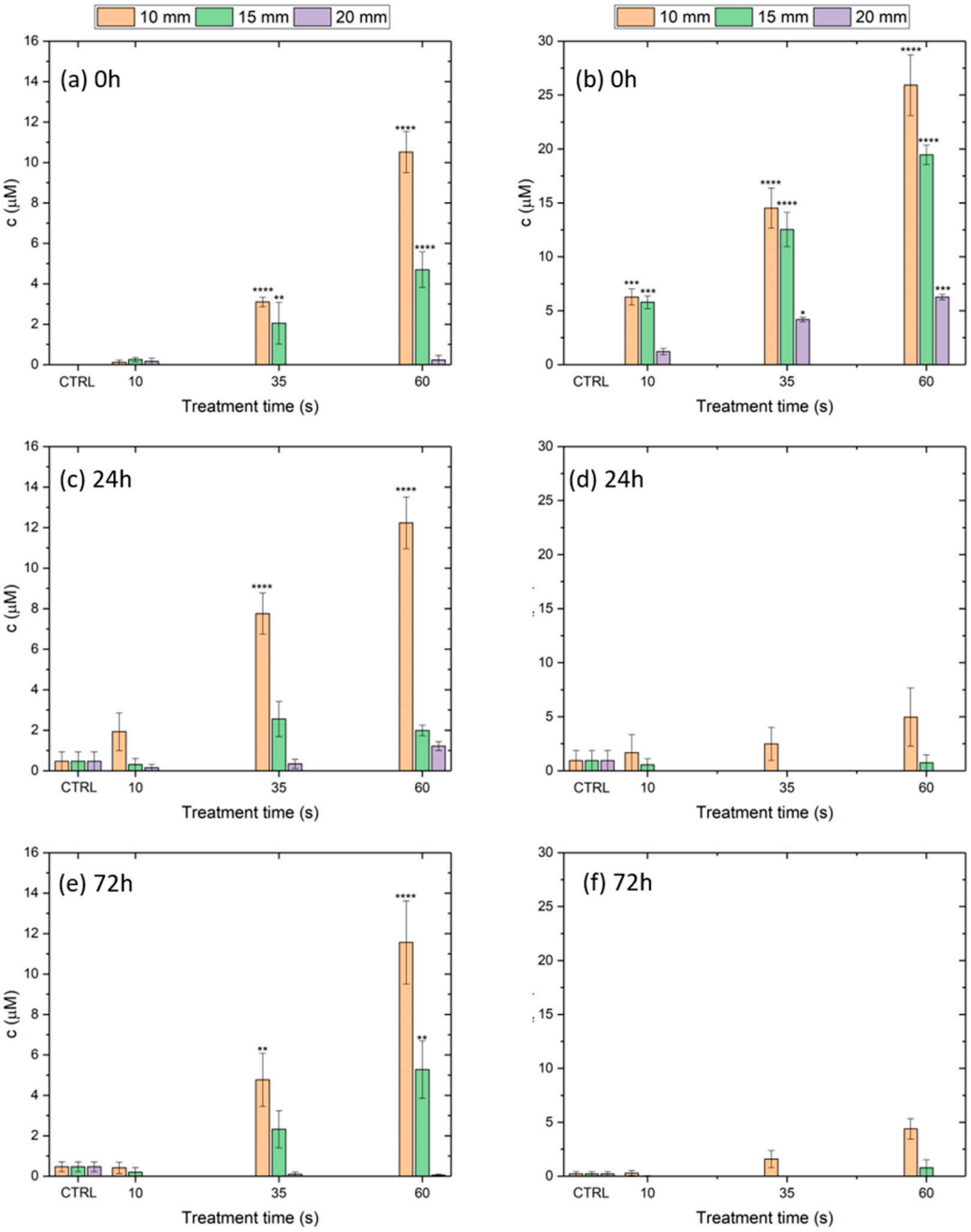

Figure 5. Concentration of NO_2^- (**left**) and H_2O_2 (**right**) in PAM measured (**a**,**b**) 0 h, (**c**,**d**) 24 h and (**e**,**f**) 72 h after plasma treatment. Results are presented as mean values ± SEM. * $p < 0.03$; ** $p < 0.002$; *** $p < 0.0002$; **** $p < 0.0001$ (two-way ANOVA, Dunnet's post-tests; n > 3).

3.3. Cell Viability

Cell viability is represented as the percentage of viable cells normalised to the control group (Figure 6) and is highly dependent on chosen parameters. As the cells were treated via direct plasma treatment, it was expected that the closest distance of 10 mm—where the plasma was in contact with the cell culture medium—would have the biggest effect on cell viability. Results show that less than 60% of cells are still viable after just 10 s of plasma treatment, and there are almost no viable cells as treatment time increases further. Consequently, greater distances, e.g., 15 mm and 20 mm, leave more viable cells in well plates. However, after just 60 s of plasma treatment, the number of viable cells dropped below 20% at a distance of 20 mm, and none were viable for shorter distances.

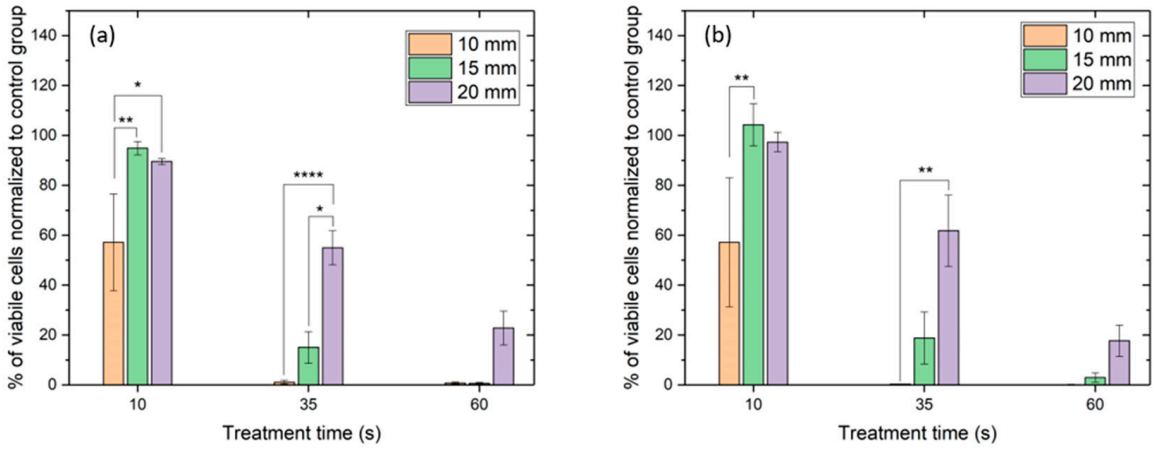

Figure 6. Cell viability test for 10 mm, 15 mm and 20 mm distance (**a**) 24 h and (**b**) 72 h after treatment. Results are presented as arithmetic mean ± SE. * $p < 0.05$; ** $p < 0.01$; **** $p < 0.0001$ (one-way ANOVA, Tukey test).

4. Discussion

Experimental results revealed that treating mouse skin cells with an atmospheric pressure kHz argon plasma jet affects cell viability. Our plasma system, used as a direct treatment, is very destructive towards L929 murine fibroblasts, highlighted by the fact that most of the cells are not viable after just 35 s of plasma treatment.

To understand what exactly causes this behaviour requires comparison with other studies and plasma systems. However, a comparison of plasma effects on cell viability with other plasma sources is extremely difficult, due to plasma source variances, plasma parameters, types of treated cells, types of plasma treatment and different approaches to the assessment of cell viability. Another problem connected to this research is repeatability, since not all researchers follow the same procedures and protocols. Similarly, researchers may not investigate all aspects needed to explain plasma effects on the treated biological samples.

Nevertheless, a comparison of approximately similar plasma systems, presented in Figure 7, highlights our plasma system's toxicity to cells. All selected sources operated in a kHz regime (20 or 40 kHz), except kINPen 09 [16], which operated in the MHz regime and was chosen as the most widely used plasma source for biomedical applications. For ease of reference, different plasma sources were given different symbols in Figure 7. The circle represents kINPen [16] (1.1 MHz, 2–6 kV, Ar—1.9 slm), the triangle represents a jet [7] (40 kHz, 4.9 kV, Ar—4 slm), the square represents a plasma torch [5] (20 kHz, 7 kV, He—5 slm), and the star represents our system. Each cited study focused on slightly different applications, so different types of cell lines were used (mHepR1, A431, HEK293, L929, LNCap, PC3 and P69). The direct approach is marked as a flat line, and the indirect approach as a dashed line. Results were selected where the distance between plasma and cell medium was 10 mm or less, and viability measured 72 h after treatment. The comparison indicates that our plasma treatment was very aggressive and the most destructive in the shortest treatment time.

To explain our jet's destructive nature on the treated cells, we must first look at the gas-phase diagnostics. OES did not show any deviation from expected species present in such plasma. The observed plasma was very stable and produced typical species for atmospheric pressure argon plasma at the beginning and end of the plasma plume (glow region) [17]. The gas temperature (measured as 318 K) is acceptable for in vitro biomedical applications and comparable to other plasma systems (e.g., kINPen 09 operates at 319–323 K [21]). Both time-resolved OES and ICCD images confirmed a regular ionisation process for a kHz-driven plasma source with the formation of pulsed streamers and filaments throughout the waveform [18–20].

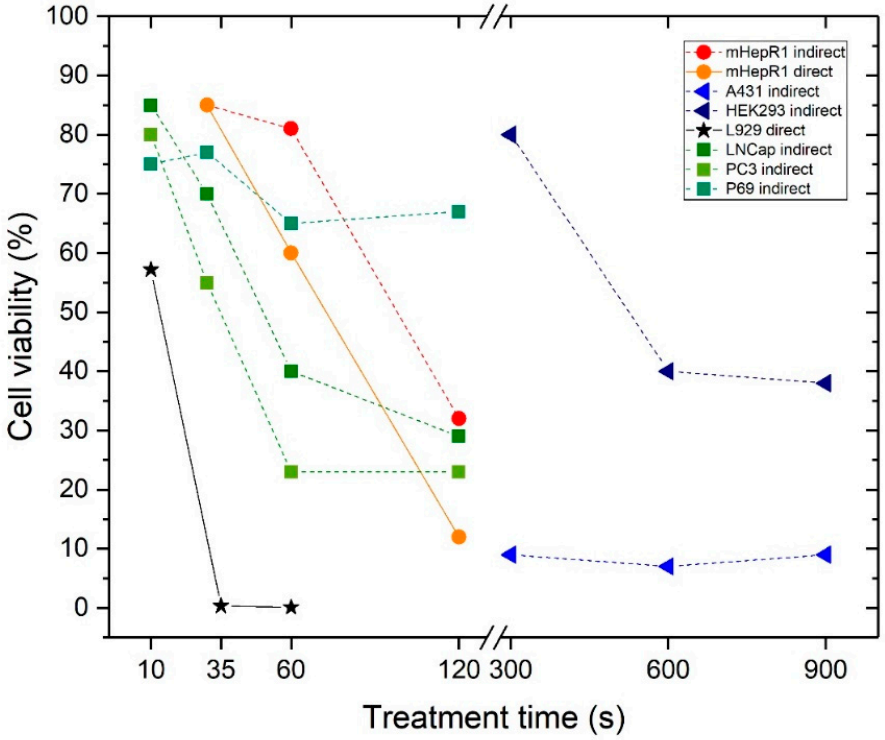

Figure 7. Comparison with other plasma sources: percentage of cell viability to direct (flat line) or indirect (dashed line) plasma treatment. Symbols represent different studies, so the circle is [16], the triangle is [7], the square is [5] and the star represents our system.

Since the gas-phase plasma parameters seem to be in accordance with other plasma sources used in cell treatment, the chemistry of the plasma-treated cell culture medium was explored. First, we made sure that the cell medium's pH and conductivity did not influence cell viability. Results were stable for all distances and treatment times. Then, we measured concentrations of NO_2^- and H_2O_2 inside the cell medium. Both concentrations were relatively low, and the NO_2^- concentration remained almost constant even 72 h after plasma treatment. In contrast, H_2O_2 concentration gradually decreased and was negligible 72 h after treatment. Comparison of H_2O_2 production with similar plasma sources is presented in Figure 8. Our results were compared to other sources that operate in the kHz region: 39.5 kHz (marked as a circle [22]), 30 kHz (marked as triangle [9]) and 17 kHz (marked as square [4]). Here, other concentrations are quite high compared to our system. One possible reason for this difference in H_2O_2 concentrations could be various cell culture media that were used; MEM was used in our research, DMEM (Dulbecco's Modified Eagle Medium) was used in [9] and RPMI 1640 was used in [22]. However, the results show that inside the same medium (DMEM), different concentrations of hydrogen peroxide can be obtained—almost a threefold difference for the longest treatment time of 60 s. Thus, we conclude that the generation of H_2O_2 is not the main source of our plasma source's destructiveness towards the L929 murine fibroblast cells. Instead, this destructiveness is thought to stem from the plasma characteristics of the argon jet used in the direct treatment conducted on these cell lines. Despite this, the argon jet is generally more aggressive towards cell lines in direct treatments than indirect ones, and as such, it should not be used for direct treatments of skin cells such as L929 murine fibroblasts.

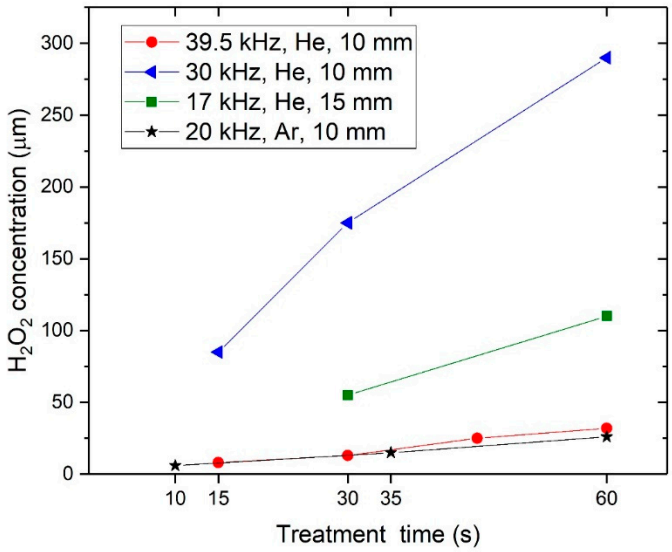

Figure 8. Comparison with other plasma sources: concentration of H_2O_2 to plasma treatment time. Symbols represent different studies: the circle is [22], the triangle is [9], the square is [4] and the star represents our system.

5. Conclusions

A non-thermal kHz argon plasma jet and its actions towards skin cells—L929 murine fibroblasts—was investigated. Although we followed reported protocols, we observed very aggressive behaviour of the jet towards the cells during direct treatment. However, neither gas-phase diagnostics nor liquid-chemistry characterisation provided a definitive answer as to why our plasma system behaved much more destructively than other sources reported. One possible reason is that such research has never been done specifically on L929 murine fibroblasts. However, there are several other possibilities for the obtained results. Firstly, plasma and its species can influence different types of cells in completely different ways. Research conducted on mHepR1 cell lines demonstrated that cell viability is higher after indirect plasma treatment than the direct approach [16]. Therefore, research must be expanded to include the indirect plasma treatment of L929 cell lines, along with additional research on other types of cells, in order to gain a deep understanding of cell behaviour. Secondly, because of the consistency of the liquid chemistry and its stability over time, it is likely that reactive species produced in the gas phase have a greater impact on cells. This is also supported by the fact that there were no major changes in viability after 24 h, from which we conclude that all cell death occurs before that time. Therefore, to gain a better insight into the timeframe for cell viability, cell viability tests—immediately or within a few hours after plasma treatment—have to be added to standard protocols. It seems that direct and short-lived plasma species could have a more extended role in cell viability than previously reported. Since this field of research is highly attractive—with many potential applications in biology and medicine—the protocols for observation of cells under plasma interaction have to be upgraded and modified.

Supplementary Materials: The following are available online at https://www.mdpi.com/2076-3417/11/3/1266/s1. Figure S1: Spatially-resolved OES with intensity normalised to 1, Figure S2: Conductivity of PAM measured right after treatment.

Author Contributions: Conceptualisation: A.J., U.C., G.S., A.N. and C.L.; Methodology: A.J., A.N. and Š.K.; Formal analysis: A.J., N.H. and Š.K.; Investigation: A.J., I.S., Š.K., A.N. and N.H.; Resources: U.C., G.S. and C.L.; Writing—original draft preparation: A.J.; writing—review and editing: G.S., N.H., I.S., Š.K. and U.C.; Visualisation: A.J.; Supervision: A.N., Š.K. and U.C.; Project administration and funding acquisition: U.C., G.S., A.N. and C.L.; All authors have read and agreed to the published version of the manuscript.

Funding: This research was funded by the Slovenian Research Agency (ARRS) and Research Foundation Flanders (FWO), grant number N3-0059 and G084917N, respectively.

Institutional Review Board Statement: Not applicable.

Data Availability Statement: The authors declare that the data supporting the findings of this study are available within the paper. All additional raw and derived data that support the plots within this paper and other finding of this study are available from the corresponding author upon reasonable request.

Conflicts of Interest: The authors declare no conflict of interest.

References

1. Laroussi, M.; Lu, X.; Keidar, M. Perspective: The physics, diagnostics, and applications of atmospheric pressure low temperature plasma sources used in plasma medicine. *J. Appl. Phys.* **2017**, *122*, 020901. [CrossRef]
2. Haertel, B.; von Woedtke, T.; Weltmann, K.D.; Lindequist, U. Non-thermal atmospheric-pressure plasma possible application in wound healing. *Biomol. Ther.* **2014**, *22*, 477–490. [CrossRef] [PubMed]
3. Laroussi, M. Plasma Medicine: A Brief Introduction. *Plasma* **2018**, *1*, 5. [CrossRef]
4. Kurita, H.; Haruta, N.; Uchihashi, Y.; Seto, T.; Takashima, K. Strand breaks and chemical modification of intracellular DNA induced by cold atmospheric pressure plasma irradiation. *PLoS ONE* **2020**, *15*, e0232724. [CrossRef] [PubMed]
5. Fofana, M.; Buñay, J.; Judée, F.; Baron, S.; Menecier, S.; Nivoix, M.; Perisse, F.; Vacavant, A.; Balandraud, X. Selective treatments of prostate tumor cells with a cold atmospheric plasma jet. *Clin. Plasma Med.* **2020**, *17–18*, 100098. [CrossRef]
6. Sato, T.; Yokoyama, M.; Johkura, K. A key inactivation factor of HeLa cell viability by a plasma flow. *J. Phys. D Appl. Phys.* **2011**, *44*, 372001. [CrossRef]
7. Schweigert, I.; Zakrevsky, D.; Gugin, P.; Yelak, E.; Golubitskaya, E.; Troitskaya, O.; Koval, O. Interaction of cold atmospheric argon and helium plasma jets with bio-target with grounded substrate beneath. *Appl. Sci.* **2019**, *9*, 4528. [CrossRef]
8. Ja Kim, S.; Min Joh, H.; Chung, T.H. Production of intracellular reactive oxygen species and change of cell viability induced by atmospheric pressure plasma in normal and cancer cells. *Appl. Phys. Lett.* **2013**, *103*, 153705. [CrossRef]
9. Gaur, N.; Kurita, H.; Oh, J.; Miyachika, S.; Ito, M.; Mizuno, A.; Cowin, A.J.; Allison, S.; Short, R.D.; Szili, E.J. On cold atmospheric-pressure plasma jet induced DNA damage in cells. *J. Phys.* **2020**, *54*, 035203. [CrossRef]
10. Jo, A.; Joh, H.M.; Chung, J.W.; Chung, T.H. Cell viability and measurement of reactive species in gas—And liquid-phase exposed by a microwave-excited atmospheric pressure argon plasma jet. *Curr. Appl. Phys.* **2020**, *20*, 562–571. [CrossRef]
11. Mehrabifard, R.; Mehdian, H.; Hajisharifi, K.; Amini, E. Improving Cold Atmospheric Pressure Plasma Efficacy on Breast Cancer Cells Control-Ability and Mortality Using Vitamin C and Static Magnetic Field. *Plasma Chem. Plasma Process.* **2020**, *40*, 511–526. [CrossRef]
12. Sremački, I.; Jurov, A.; Modic, M.; Cvelbar, U.; Wang, L.; Leys, C.; Nikiforov, A. On diagnostics of annular-shape radio-frequency plasma jet operating in argon in atmospheric conditions. *Plasma Sources Sci. Technol.* **2020**, *29*, 035027. [CrossRef]
13. Schieber, M.; Chandel, N.S. ROS function in redox signaling and oxidative stress. *Curr. Biol.* **2014**, *24*, R453–R462. [CrossRef] [PubMed]
14. Clément, M.V.; Pervaiz, S. Intracellular superoxide and hydrogen peroxide concentrations: A critical balance that determines survival or death. *Redox Rep.* **2001**, *6*, 211–214. [CrossRef]
15. Duchesne, C.; Frescaline, N.; Lataillade, J.J.; Rousseau, A. Comparative study between direct and indirect treatment with cold atmospheric plasma on in vitro and in vivo models of wound healing. *Plasma Med.* **2018**, *8*, 379–401. [CrossRef]
16. Hoentsch, M.; Von Woedtke, T.; Weltmann, K.D.; Barbara Nebe, J. Time-dependent effects of low-temperature atmospheric-pressure argon plasma on epithelial cell attachment, viability and tight junction formation in vitro. *J. Phys. D Appl. Phys.* **2012**, *45*, 025026. [CrossRef]
17. Jonkers, J.; Van De Sande, M.; Sola, A.; Gamero, A.; Van Der Mullen, J. On the differences between ionizing helium and argon plasmas at atmospheric pressure. *Plasma Sources Sci. Technol.* **2003**, *12*, 30–38. [CrossRef]
18. Laroussi, M.; Begum, A.; Karakas, E. Experimental investigations of plasma. *J. Phys. D Appl. Phys.* **2009**, *42*, 055207. [CrossRef]
19. Jarrige, J.; Laroussi, M.; Karakas, E. Formation and dynamics of plasma bullets in a non-thermal plasma jet: Influence of the high-voltage parameters. *Plasma Sources Sci. Technol.* **2010**, *19*, 065005. [CrossRef]
20. Barletta, F.; Leys, C.; Colombo, V.; Gherardi, M.; Britun, N.; Snyders, R.; Nikiforov, A. Insights into plasma-assisted polymerization at atmospheric pressure by spectroscopic diagnostics. *Plasma Process. Polym.* **2020**, *17*, 1–15. [CrossRef]
21. Bekeschus, S.; Schmidt, A.; Weltmann, K.D.; von Woedtke, T. The plasma jet kINPen—A powerful tool for wound healing. *Clin. Plasma Med.* **2016**, *4*, 19–28. [CrossRef]
22. Xu, G.M.; Hao, Y.; Sun, M.Y.; Liu, J.R.; Shi, X.M.; Zhang, G.J. Characteristics of Plasma Activated Medium Produced by Atmospheric Pressure Helium Plasma Jet and Its Selective Effect on Malignant Melanoma and Normal Fibroblast Cells. *IEEE Trans. Plasma Sci.* **2020**, *48*, 587–595. [CrossRef]